Molecular Therapy
Methods & Clinical Development
Original Article

Production of recombinant adeno-associated virus 5 using a novel self-attenuating adenovirus production platform

Matthew K. Roach,[1] Phillip Wirz,[1] Jeremy Rouse,[1] Allison Schorzman,[1] Clayton W. Beard,[1] and David Scott[1]

[1]BridgeBio Gene Therapy LLC, Raleigh, NC 27607, USA

Recombinant adeno-associated virus (rAAV) has become a prominent vector for clinical use. Despite an increase in successful clinical outcomes, the amount of high-quality rAAVs required for clinical trials and eventual commercial demand is difficult to produce, especially for genetic diseases that are prevalent or require high doses. Many groups are focused on establishing production processes that can produce sufficient rAAV while maintaining potency and quality. Our group used a novel production platform to increase our yield of rAAV5. This production platform uses tetracycline-enabled self-silencing adenovirus (TESSA) to deliver the wild-type AAV replication and capsid genes alongside the adenovirus helper genes necessary for production. Here, we describe our efforts to evaluate the TESSA platform in house. We conducted numerous experiments to determine the optimal conditions for producing rAAV5 from the TESSA production system. We then produced rAAV5 from the TESSA system to compare against rAAV5 produced from triple transfection. Ultimately, we generated data that showed that the vector genome yield of rAAV5 produced with TESSA was >20-fold higher than rAAV5 produced with triple transfection. Additionally, our data show that quality as well as potency in mice of rAAV5 produced with the TESSA system and by triple transfection are equivalent.

INTRODUCTION

Recombinant adeno-associated virus (rAAV) has become a popular vector for clinical use.[1] The parvovirus is capable of transduction of many different tissues and can deliver cargo for sustained expression.[2] Given the widespread use of rAAV for gene therapies, an increasing amount of emphasis has been placed on the manufacturing processes used to produce the vector.[3] The emphasis has led to a realization that the yield, quality, and scalability of the vector must be improved as the production processes move toward clinical and commercial supply. One recent improvement in the manufacture of rAAV includes the development of anion exchange chromatography for the separation of empty capsids from the desired full capsids replacing non-scalable ultracentrifugation processes.[4,5] Other authors have described the implementation of various viral systems to boost productivity, including helper viral systems such as baculovirus or herpes simplex virus.[6,7] While the baculovirus Sf9 system has demonstrated impressive rAAV yields, production of rAAV in a non-mammalian cell line has led to probes into post-translational modifications, which shows significant differences from rAAV produced by the triple transfection process using HEK293 cells.[8] Recent publications have reported a decrease in the incorporation of viral proteins (VPs) 1 and 2, increased deamidation, and decreased potency from baculovirus SF9-derived AAV vectors.[9] Furthermore, the transfection reagents used for traditional triple transfection processes are known to have time-sensitive complexation, which can lead to decreases in yield as the process is scaled up, as large transfection volumes have to be fed into bioreactors in a timely manner. Thus, there is a need for a system that achieves efficient delivery of all the components needed to produce recombinant AAV while producing quality particles out of a mammalian system.

Recently, OXGENE has reported on the use of a self-attenuating adenovirus-based production system that can manufacture AAV at yields much higher than that of the traditional triple transfection process.[10] The system, entitled tetracycline-enabled self-silencing adenovirus (TESSA), relies on an E1/E3-deleted adenovirus type 5 vector genome that has been modified to encode a tetracycline operator within the major late promoter and a repressor positioned downstream under the transcription of the major late promoter. The modified adenovirus genome also encodes the AAV2 rep sequence alongside the desired AAV cap sequence. In the presence of doxycycline, the TESSA vector can replicate in HEK293 cells to produce a seed stock for use in eventual AAV production. Conversely, in the absence of doxycycline, TESSA is unable to produce its structural capsid proteins and replicate (i.e., no adenovirus replication during AAV production). The use of a non-replicating helper virus alleviates some of the residual virus concerns of previous adenovirus helper systems. The TESSA production system has two distinct approaches that can be used to produce AAV. One of the approaches, TESSA 2.0, uses one TESSA vector to deliver the adenovirus helper genes, AAV2 Rep, and AAV5 Cap, while a second TESSA vector delivers the adenovirus helper genes alongside the transgene of interest (GOI). Alternatively, in the work

Received 23 May 2024; accepted 9 August 2024;
https://doi.org/10.1016/j.omtm.2024.101320.

Correspondence: Matthew K Roach, BridgeBio Gene Therapy LLC, Raleigh, NC 27607, USA.
E-mail: matt.roach@bridgebio.com

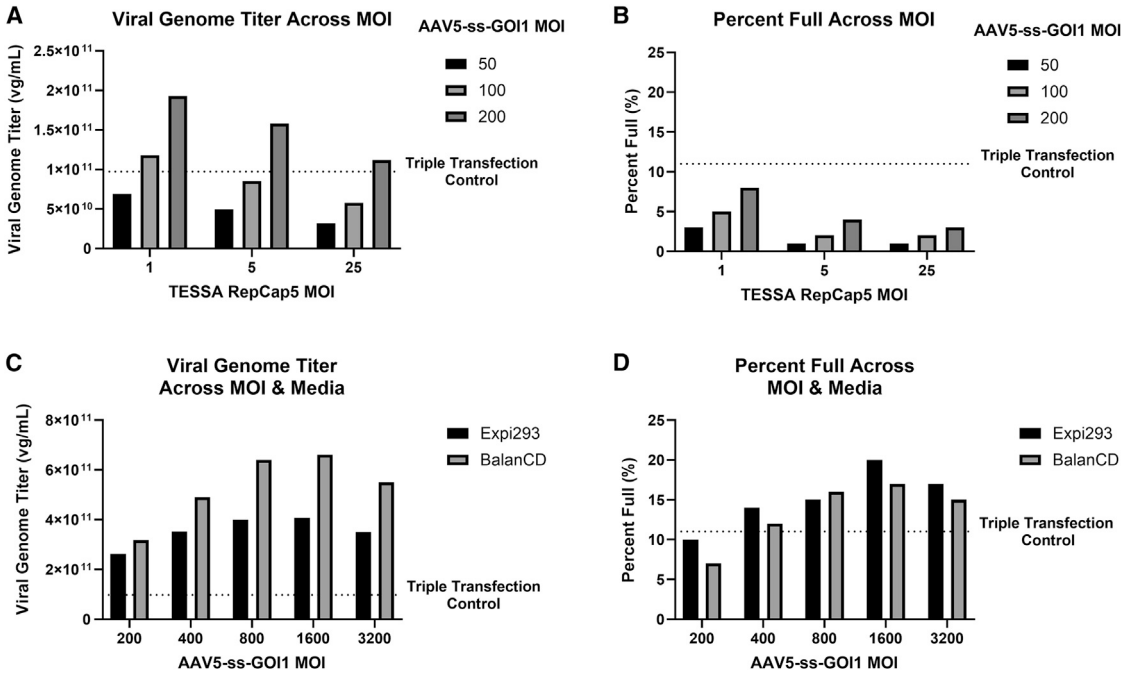

Figure 1. Initial optimization of TESSA system with AAV5-ss-GOI1

(A and B) HEK293 cells were transduced with TESSA-RepCap5 at an MOI of 1, 5, and 25 TCID50/cell in combination with AAV5-ss-GOI1 at an MOI of 50, 100, and 200 to determine the optimal MOI combinations for viral genome production (A) and percentage of full capsids (B). The segmented line on both graphs demonstrates the viral genome titer and percentage of full capsids for the triple transfection control ($n = 2$). (C and D) HEK293 cells were grown and cultured with Expi293 or BalanCD media before co-infection using TESSA-RepCap5 at an MOI of 1 with AAV5-ss-GOI1 used at an MOI range of 200–3,200 for assessment of viral genome production (C) and percentage of full capsids (D). The segmented line on both graphs demonstrates the viral genome titer and percentage of full capsids for the triple transfection control ($n = 2$).

presented here, we used the TESSA Pro approach, in which one TESSA vector delivers the adenovirus helper, AAV2 Rep, and AAV5 Cap, while the transgene is delivered by a recombinant AAV. This allowed for a decrease in the number of TESSA vectors (i.e., for delivery of the transgene) needed to initiate rAAV production.

We showed that the novel TESSA Pro system can be optimized to produce high-yielding rAAV irrespective of the transgene. Additionally, we demonstrated that the optimized TESSA system produces a greater proportion of full AAV5 capsid particles at the lysate stage, eventually leading to a final product with a higher percentage of full capsids than rAAV5 produced from traditional triple transfection. We explored numerous other analytics including residual HEK293 host cell DNA, post-translational modifications via mass spectrometry, and *in vitro* potency. Finally, we showed equivalent murine *in vivo* potency of the TESSA-produced rAAV5 as compared with a triple transfection-produced rAAV5 carrying the same transgene.

RESULTS

Screening of the TESSA system with AAV5-ss-GOI1

We used the TESSA Pro version of the TESSA system, which uses the delivery of RepCap via the TESSA vector (TESSA-RepCap5) and delivery of the GOI via rAAV (in our case, rAAV5). Single-stranded GOI1 (ss-GOI1) is a transgene with a total length of 4544 base pairs (bp), including the AAV2 inverted terminal repeats. We screened TESSA-RepCap5 and AAV5-ss-GOI1 at various multiplicities of infection (MOI) for transduction in a suspension HEK293 cell line using 125-mL shake flasks containing 30 mL cell culture. The resulting lysates from these shake flasks were harvested 72 h after transduction and tested for viral genome titer via digital droplet PCR (ddPCR) and capsid titer via ELISA. Our data show that the production of AAV5-ss-GOI1 at relatively high viral genome titers was possible with the TESSA production system. The TESSA system was able to generate 1.93E+11 viral genomes (vg)/mL (Figure 1A) and 8% full capsid particles (Figure 1B).

Subsequent experiments tested MOIs ranging from 200 to 3,200 for AAV5-ss-GOI1 and cultured with two different commercially available media (Thermo Fisher Scientific Expi293 and Irvine Scientific BalanCD). An MOI of 1 TCID50/cell for TESSA-RepCap5 was used in all conditions. The highest viral genome titers were observed for AAV5-ss-GOI1 at an MOI of 1,600 independent of media conditions (Figure 1C). Interestingly, an increase in viral genome titer was observed for the BalanCD media when compared with the Expi293 media at each AAV5-ss-GOI1 MOI; therefore, BalanCD media was used in subsequent production studies. The percentage of full capsids was comparable between the two media (Figure 1D). Furthermore, we also observed an increase in the proportion of full capsids (>15% full) for both media conditions as AAV5-ss-GOI1 was increased to an MOI of 1,600. The viral genome titers for both the 800 and

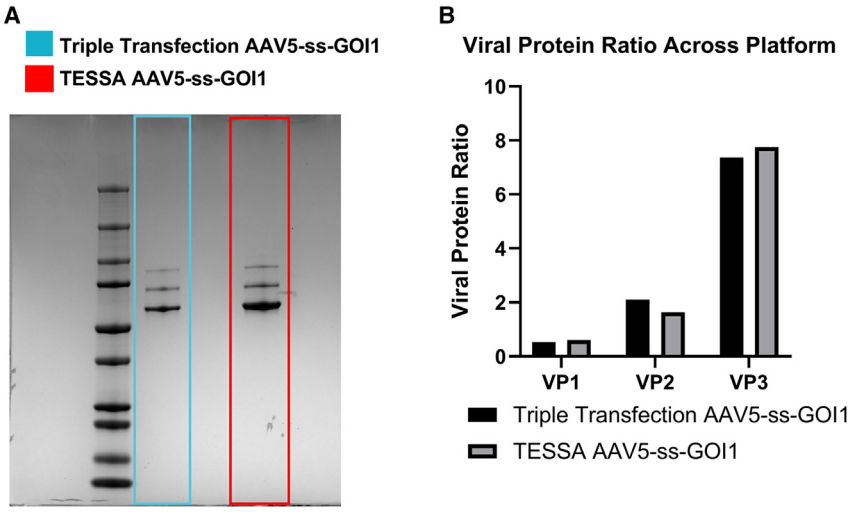

Figure 2. Comparison of VP Ratio for Triple Transfection and TESSA Produced AAV5-ss-GOI1

(A) SDS-PAGE gel; protein ladder in the leftmost lane followed by triple transfection produced AAV5-GOI1 then TESSA produced AAV5-GOI1. (B) Graph of the densitometry of the SDS-PAGE gel comparing VP ratio across rAAV5 produced from both systems.

1,600 AAV5-ss-GOI1 MOI conditions reached >6E+11 vg/mL in BalanCD media, which was a 6-fold increase in viral genome titer compared with the triple transfection control.

Therefore, we further examined AAV5-ss-GOI1 MOIs between 800 and 1,600 (Figure S1). Titers ranged between 5.6E+11 and 6.8E+11 vg/mL with the highest producing AAV5-ss-GOI1 MOI observed from the 1,400 condition.

Based on these results, we scaled up rAAV production using an AAV5-ss-GOI1 MOI of 1,400 and a TESSA-RepCap5 MOI of 1 in BalanCD media and purified it via affinity chromatography. After purification, we assessed the VP ratios between traditional triple transfection produced AAV5-ss-GOI1 and TESSA-produced AAV5-ss-GOI1 (Figures 2A and 2B). VP composition in the AAV capsid is important as reduced incorporation of VP1 can result in a reduction in AAV potency.[9] The SDS-PAGE gel demonstrated comparable amounts of VP1, VP2, and VP3 proteins from both the AAV5-ss-GOI1 produced from the TESSA system and AAV5-ss-GOI1 produced from the triple transfection system.

Optimization of TESSA production of AAV5-sc-GOI2

After demonstrating the potential of the TESSA system, we sought to ensure that the increased productivity was not transgene specific or restricted to single-stranded AAV genomes. To test this, we produced rAAV5 containing sc-GOI2. The sc-GOI2 construct encodes a transgene within a self-complementary AAV genome and has a total length of 1,882 bp. Furthermore, sc-GOI2 contains a different promoter and GOI compared with ss-GOI1. We tested several conditions with variable TESSA RepCap5 MOI and AAV5-sc-GOI2 MOI. Lysates were tested for viral genome titer via ddPCR and capsid titer via capsid ELISA.

We observed viral genome titers approaching 2E+12 vg/mL (Figure 3A). An MOI of 2,800 vg/cell for AAV5-sc-GOI2 and an MOI of 3 TCID50/cell for TESSA-RepCap5 generated the highest viral genome titer of 1.94E+12 vg/mL. This was more than a 20-fold yield increase from our typical triple transfection process for the same AAV5-sc-GOI2 construct. Interestingly, even the lowest producing condition generated a viral genome titer of 1.37E+12 vg/mL, 15-fold that of our triple transfection control.

While the viral genome titer peaked at a TESSA-RepCap5 MOI of 3 independent of AAV5-sc-GOI2 MOI, we observed a consistent trend that the percentage of full capsids decreased as the MOI of TESSA-RepCap5 was increased at each AAV5-sc-GOI2 MOI (Figure 3B). Generally, AAV5-sc-GOI2 used at an MOI of 2,800 generated the highest percentage of full capsids, but all MOI conditions yielded a relatively high proportion of full capsids given that these were upstream lysates. Impressively, percentage of full capsids for TESSA-produced AAV5-sc-GOI2 were 3- to 4-fold higher than our triple transfection control produced AAV5-sc-GOI2.

Comparison of TESSA and triple transfection processes

To ensure scalability of the TESSA platform, we increased our production 66-fold (2 L) using AAV5-sc-GOI2 at an MOI of 2,800 and TESSA-RepCap5 at an MOI of 3. Additionally, 20 L of AAV5-sc-GOI2 was produced through triple transfection to compare to the TESSA-produced AAV5-sc-GOI2. The lysate from each production was processed through clarification, affinity chromatography, anion-exchange chromatography, buffer exchange, and sterile filtration. Process recovery details are shown in Table 1. The TESSA lysate viral genome titer was 1.45E+12 vg/mL compared with a triple transfection lysate viral genome titer of 7.08E+10 vg/mL, representing a 20.5-fold increase. Recovery of viral genomes from affinity chromatography were comparable between the two platforms. Both affinity and anion-exchange chromatograms were generated for the TESSA-produced AAV5-sc-GOI2 and triple transfection produced AAV5-sc-GOI2 (Figures 4A and 4B). The affinity chromatogram for the triple transfection production has been segmented to show the elution and subsequent cleaning at a reasonable scale. The previously mentioned increase in viral genome titer for the TESSA system is evident from observation of the loads of the two runs. The TESSA affinity chromatography run had a load of approximately 2 L of clarified lysate while the triple transfection affinity chromatography run had 10-fold the volume of clarified lysate loaded. Despite a large difference in the amount loaded, the TESSA and triple transfection elution peak areas were comparable.

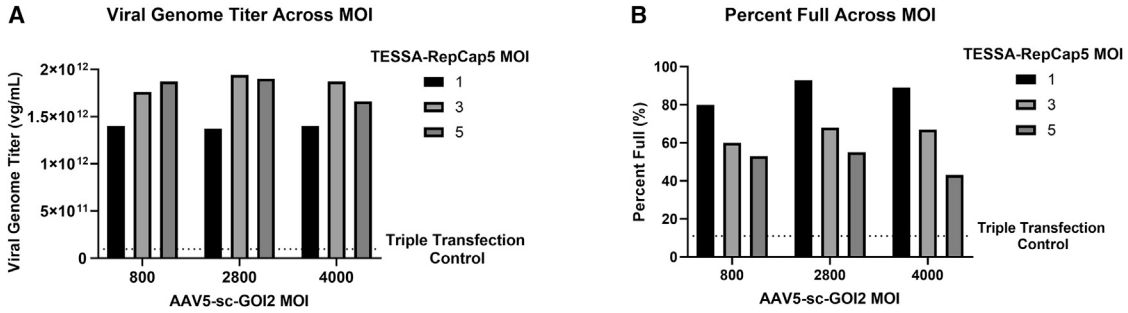

Figure 3. Optimization of the TESSA platform for AAV5-sc-GOI2

(A and B) HEK293 cells were transduced with TESSA-RepCap5 at an MOI of 1, 3, and 5 TCID50/cell in combination with AAV5-sc-GOI2 at MOIs of 800, 2,800, and 4,000 to determine the optimal MOI combinations for viral genome production (A) and percentage of full capsids (B). The segmented line on both graphs demonstrates the viral genome titer and percentage of full capsids for the triple transfection control (n = 2).

Recovery of viral genomes across the anion-exchange chromatography step favored the TESSA system (64% vs. 55%). For the anion-exchange chromatograms, both the TESSA and triple transfection chromatograms are shown at the same scale (Figure 4B). The first peak shown in both chromatograms represents a portion of the empty capsid population and the full peak is marked by the crossover of UV260 above UV280. When comparing the TESSA and triple transfection chromatograms, the empty peak is distinctively much larger for the triple transfection produced material. Consistent with this observation, the full peak is larger for the TESSA AAV5-sc-GOI2, likely indicating a higher percentage of full capsids. We typically observe a third "aggregate" peak in our anion-exchange step that can be seen between the full peak and 1 M sodium chloride strip peak on the triple transfection chromatogram. Interestingly, this aggregate peak was not observed from the TESSA-produced material.

The total process recovery was slightly greater for the TESSA platform at 55% vs. 50% for the triple transfection system. Post-purification, the TESSA system generated double the amount of AAV5-sc-GOI2 as the triple transfection system despite using 10-fold less cell culture volume. Ultimately, the process recoveries were similar, while the productivity for the TESSA system was much higher than the triple transfection system.

Assessment of the percentage of full capsids was conducted at each step of the production process by dividing the ddPCR viral genome titer by capsid ELISA titer (Table 2). The percentage of full capsids for AAV5-sc-GOI2 produced through the TESSA system was higher than that of AAV5-sc-GOI2 produced through triple transfection throughout the entire process. TESSA AAV5-sc-GOI2 capsids at the lysate stage were measured at 37% full, while the triple transfection AAV5-sc-GOI2 capsids at the lysate stage were measured at 9% full. After anion exchange, the TESSA AAV5-sc-GOI2 material was enriched to 91% full capsids, while the triple transfection AAV5-sc-GOI2 anion-exchange eluate was determined to be 51% full capsids. The proportion of full rAAV capsids from the final TESSA-produced material was almost double compared with the triple transfection system (100% vs. 51%).

Residual host cell DNA is commonly measured for fully purified rAAV, as the introduction of residual host cell DNA can lead to an increased risk of infection for patients. We measured residual host cell DNA for AAV5-sc-GOI2 produced through the TESSA and triple transfection systems to ensure the TESSA produced rAAV was comparable with or lower than the triple transfection produced rAAV. Final AAV5-sc-GOI2 from the TESSA production system showed a 5.9-fold lower residual host cell DNA than AAV5-sc-GOI2 produced through the triple transfection system (Table 2). This difference in

Table 1. Viral genome recovery for TESSA and triple transfection platforms

Process	Process step	Viral genome titer (vg/mL)	Volume (mL)	Viral genome yield (vg)	Viral genome recovery (%)
TESSA	Lysate	1.45E+12	2000	2.90E+15	100%
	Affinity Eluate	2.38E+13	110	2.62E+15	90%
	Anion-Exchange Eluate	3.17E+12	583	1.85E+15	64%
	Final Material	4.88E+13	32.5	1.59E+15	55%
Triple Transfection	Lysate	7.08E+10	22750	1.61E+15	100%
	Affinity Eluate	1.30E+13	110	1.43E+15	89%
	Anion-Exchange Eluate	1.85E+12	474	8.77E+14	55%
	Final Material	4.59E+13	17.7	8.10E+14	50%

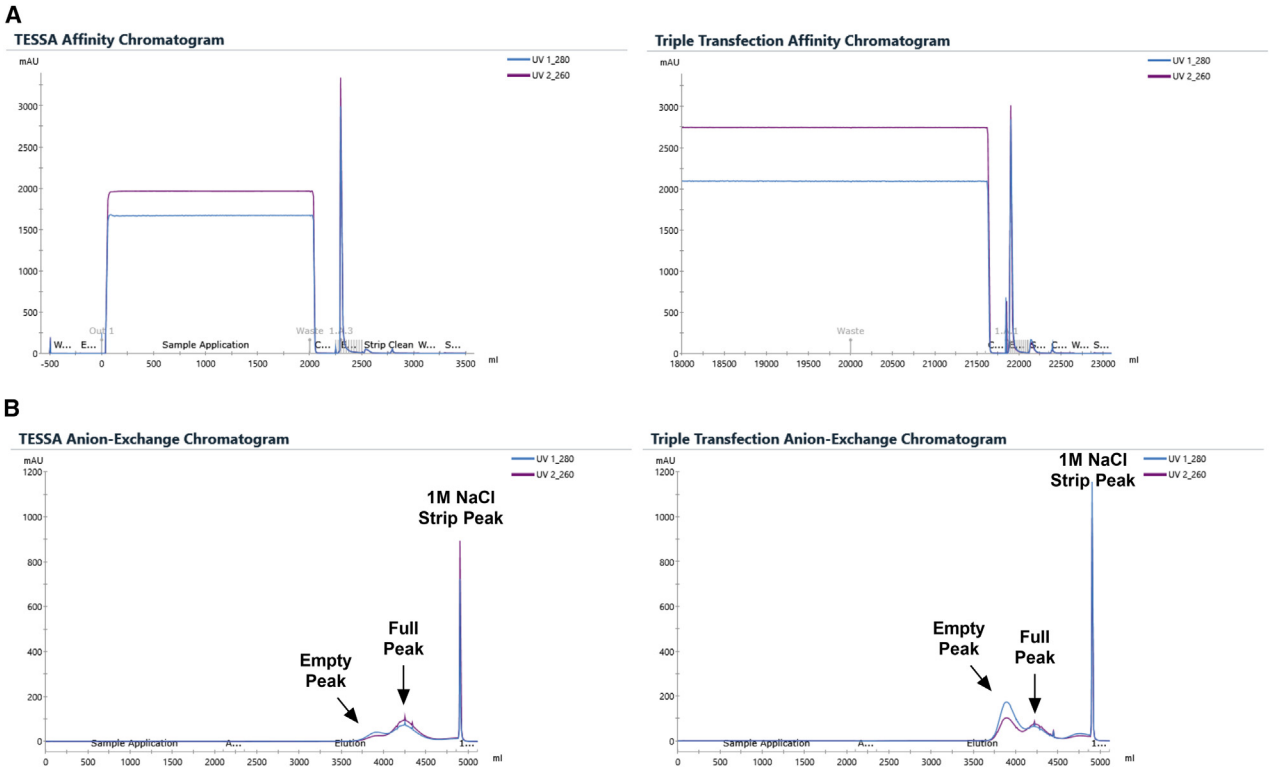

Figure 4. Chromatograms for TESSA and triple transfection purification

(A) UV280 and UV260 affinity chromatogram for TESSA-produced AAV5-sc-GOI2 (left) and triple transfection-produced AAV5-sc-GOI2 (right). (B) UV280 and UV260 anion-exchange chromatogram for TESSA-produced AAV5-sc-GOI2 (left) and triple transfection-produced AAV5-sc-GOI2 (right).

residual host cell DNA can likely be attributed to the higher productivity of the TESSA system achieved while at relatively low cell density.

Analysis of post-translational modifications for TESSA and triple produced samples

AAV5-ss-GOI3 expresses the same GOI as ss-GOI1, but had the promoter swapped to boost production yields (Figure S2). rAAV samples were analyzed via mass spectrometry to determine if the rAAV produced through the two platforms demonstrated any differences in post-translational modifications, an additional analysis that needs to be monitored for potential effects on potency of the vector (Table S1). Both TESSA and triple transfection produced AAV5-sc-GOI2 and AAV5-ss-GOI3 samples were tested for acetylation, deamidation, methylation, oxidation, and phosphorylation. High sequence coverage was achieved for all samples (between 97.9% and 100% coverage for VP1, VP2, and VP3). No differences in acetylation were observed. AAV5-sc-GOI2 produced by triple transfection had the highest amount of deamidation at the N55 site, which is a residue that is commonly deamidated in AAV5 preparations and is associated with a decrease in potency.[11,12] Specifically, the AAV5-sc-GOI2 triple transfection sample had more than double the amount of N55 deamidation compared with TESSA produced AAV5-sc-GOI2 (16.5% vs. 7.4%, respectively). All other residues tested had less than 2.5% relative abundance of deamidation. AAV5-ss-GOI3 produced from triple transfection and TESSA followed the same deamidation trend with the triple transfection sample having double the abundance compared with the TESSA-derived material. None of the other residues tested had more than 1.8% deamidation for either sample. Ten residues were observed for methylation, although none of the sites for either set of samples had more than 0.6% methylation. Modifications by oxidation and phosphorylation were found to be comparable between AAV5 materials produced from the TESSA and triple transfection process.

In vitro and *in vivo* potency assessments

To assess potential differences in potency between TESSA-produced AAV5 and traditional triple transfection-produced AAV5, HeLaRC32 cells were transduced with rAAV5 from each production platform at MOIs ranging from 3,125 to 200,000 and mRNA production was assessed by RT-qPCR. TESSA-derived AAV5-sc-GOI2 had comparable potency with AAV5-sc-GOI2 produced by triple transfection (Figure 5A). Interestingly, when another batch of TESSA-produced material, AAV5-ss-GOI3, was tested under the same paradigm, there was a slight decrease in potency compared with the triple transfection produced AAV5-ss-GOI3. Combined, these results show that TESSA-produced rAAV5 is equally potent compared with the triple transfection produced AAV5 and warranted additional testing in animals.

Table 2. Comparison of percentage of full capsids and residual host cell DNA

Process	Process step	Percentage of full capsids (%)	Residual host cell DNA (ng/1E13 vg)
TESSA	lysate	37	–
	affinity eluate	52	–
	anion-exchange eluate	91	–
	final material	100	167
Triple transfection	lysate	9	–
	affinity eluate	11	–
	anion-exchange eluate	51	–
	final material	51	982

The same material was used for *in vivo* potency assessment and introduced to 6-week-old C57Bl/6J mice via tail vein injection at a dose of 5×10^{13} vg/kg (Figure 6). Four weeks after injection the liver, adrenal glands, heart, and brain were collected for assessment of vector genomes and transgene RNA expression. Similar levels of vector genomes were found in tissues receiving either AAV5-sc-GOI2 or AAV5-ss-GOI3 when the material was produced by TESSA or triple transfection (Figures 6A and 6C). Further, these similar levels of vector genomes led to near equal levels of transgene RNA production (Figures 6B and 6D). Overall, the *in vitro* and *in vivo* potency assessment demonstrated that TESSA-produced AAV has comparable potency to triple transfection-produced AAV.

DISCUSSION

The primary goal of process development groups across the AAV space has been to increase the viral genome yield and quality of the vectors eventually intended for clinical use. The TESSA Pro production system trialed throughout this work demonstrates the ability of this system to generate more rAAV than traditional triple transfection while maintaining key quality attributes (i.e., percentage of full capsids, VP ratio, residual host cell DNA, and potency).

Ultimately, the success of rAAV as a gene therapy depends on the ability to produce the vector economically. The production of rAAV has traditionally been accomplished by triple transfection, which can be costly due to the amount of transfection reagent and plasmid DNA required to efficiently deliver the required genes into the production cells. Additionally, triple transfection can lead to inefficient delivery as it requires delivery of three separate plasmids into each cell to produce AAV. Our results could indicate that the delivery of AAV components is better accomplished using a helper virus system, in which some or all components necessary for AAV production can be packaged into one or two viruses, which have been naturally evolved to infect host cells. In our case, the use of a modified adenovirus to deliver cargo may allow for more efficient delivery, as the AAV carrying the GOI is paired with its natural helper virus. Additionally, the use of a modified adenovirus containing most of the original helper virus genes may allow for a more productive host environment by dampening the innate immune response of the host cell to the replication and capsid genes of AAV.[13] Together these benefits of using a helper virus production system allow for more economic production of AAV, which in turn increases the likelihood of meeting clinical and commercial demand.

Our initial trial of the TESSA Pro system began with the screening of MOI for both the TESSA-RepCap5 carrying the adenovirus helper genes and the AAV5-ss-GOI1 carrying our GOI. It was quickly evident that the optimal MOI required for AAV5-ss-GOI1 was higher than we initially anticipated, although the initial results reached a high titer of nearly 2E+11 vg/mL. We then tested an increase in AAV5-ss-GOI1 MOI while maintaining the TESSA-RepCap5 MOI and achieved viral genome titers 3-fold higher than our initial results, while doubling the percentage of full capsids. Our initial work found that an MOI between 800 and 1,600 was optimal for AAV5-ss-GOI1, although it is likely that a different AAV capsid serotype could be used to reduce the amount of rAAV needed as a starting material. Reports on the *in vitro* transduction of AAV serotypes indicate that AAV2 or AAV6 can transduce HEK293 cells more efficiently than AAV5.[14] While this type of optimization would be critical for formalizing a commercial process it was outside the scope of the current work and thus not investigated. Overall, the limited screening of MOI and growth media led to high rAAV5 viral genome titer production and appropriate level of packaging when compared with historical results.

Our SDS-PAGE of AAV5-ss-GOI1 produced through both TESSA and triple transfection showed that the VP ratios were similar. This was an important assessment on rAAV5 produced from the TESSA platform, as previous studies have shown that loss or reduction of the VP1 protein can decrease potency.[15,16] Additionally, it was promising to observe comparable amounts of VP2 as the overexpression of VP2 has been reported to drive altered rAAV capsid protein stoichiometry.[17]

One of our initial objectives was to ensure that the TESSA production system could be used as a platform, ideally generating consistently high rAAV5 viral genome yields across various transgenes. Interestingly, the viral genome titers generated using AAV5-sc-GOI2 were higher than those from the AAV5-ss-GOI1 production. We hypothesized that this could be due to the difference in promoters used for these constructs, possibly due to high transcriptional activity or transgene expression that may hinder AAV replication. Ultimately, we found that swapping the promoter for ss-GOI1 to a new promoter (GOI named ss-GOI3) boosted rAAV5 viral genome titers to levels matching sc-GOI2 for the TESSA production system (Figure S2). We also tested this for triple transfection and found a similar relative boost in rAAV5 vector genome productivity. The ss-GOI3 was then used for subsequent *in vitro* potency experiments (Figure 5) and *in vivo* potency experiments (Figure 6). After confirming the validity of the TESSA platform across three separate constructs, we demonstrated that the TESSA Pro platform could be scaled up and the rAAV5 produced through the system was purified through our

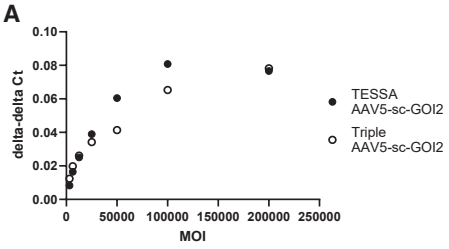

MOI	AAV5-sc-GOI2 TESSA vs Triple
3125	72%
6250	88%
12500	100%
25000	117%
50000	150%
100000	126%
200000	99%
Average	107%

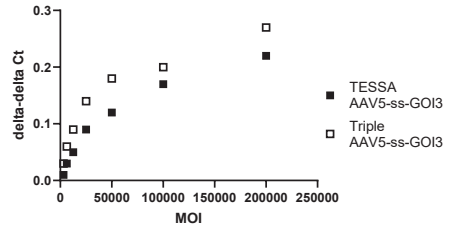

MOI	AAV5-ss-GOI3 TESSA vs Triple
3125	47%
6250	45%
12500	55%
25000	65%
50000	68%
100000	83%
200000	79%
Average	63%

Figure 5. In vitro potency comparison across production methods

(A) *In vitro* potency assay comparing TESSA produced AAV5-sc-GOI2 and triple transfection-produced AAV5-sc-GOI2. (B) *In vitro* potency assay comparing TESSA produced AAV5-ss-GOI3 and triple transfection-produced AAV5-ss-GOI3.

standard purification process. Overall, we found that the TESSA Pro platform outperformed our triple transfection process in each assessment (i.e., viral genome yield, percentage of full capsids, residual host cell DNA). The increased rAAV5 productivity achieved with the TESSA Pro platform suggests that the platform could aid in alleviating the bottleneck of rAAV production for clinical and commercial use.

rAAV5 viral genome titers greater than 1.9E12 vg/mL were achieved while still using a low cell density culture. Assumedly, higher rAAV5 viral genome titers may be achievable through intensification of the cell culture process (i.e., increasing viable cell density at the time of transduction or use of perfusion to remove cell waste).[11] While our primary goal was to determine if the TESSA system could produce higher rAAV5 viral genome titers than our triple transfection system, we found that the percentage of full capsids was also considerably higher at the lysate stage for AAV5-sc-GOI2. Interestingly, we observed that the TESSA-produced AAV5-ss-GOI1 had a similar percentage of full capsids as compared with AAV5-ss-GOI1 produced through the triple transfection process, suggesting that differences in transgene may affect the percentage of full capsids, similar to traditional AAV production platforms. While we observed differences in the percent of full capsids and viral genome titer across different constructs, in both cases, the optimized conditions for the TESSA platform outperformed the triple transfection system.

We compared post-translational modifications for the TESSA and triple transfection production samples for both AAV5-sc-GOI2 and AAV5-ss-GOI3. Previous studies have shown that switching production systems can cause significant differences in post-translational modifications.[8] Our initial interest in the TESSA platform was piqued by the use of the HEK293 cell line for the TESSA production system, which is also used in the triple transfection platform. We hypothesized that some of the differences in rAAV post-translational modifications seen in other production systems, such as the baculovirus SF9 systems, could be avoided by using the same cell line as in our triple transfection platform. Interestingly, we observed an increase in deamidation across the N55 residue for the rAAV5 triple transfection produced material when compared with TESSA-produced rAAV5. The deamidation of the rAAV5 N55 residue has previously been reported to affect potency.[12,18] This suggests that the TESSA platform may be less likely to induce deamidation for the rAAV5 N55 residue when compared with the triple transfection platform and maintain particle potency. No other large differences in rAAV5 post-translational modifications were observed between the TESSA and triple production methods across either of the GOIs tested.

After confirming that rAAV5 produced through the TESSA production platform achieved higher yields than rAAV5 produced through the triple transfection system, our evaluation shifted to ensuring that

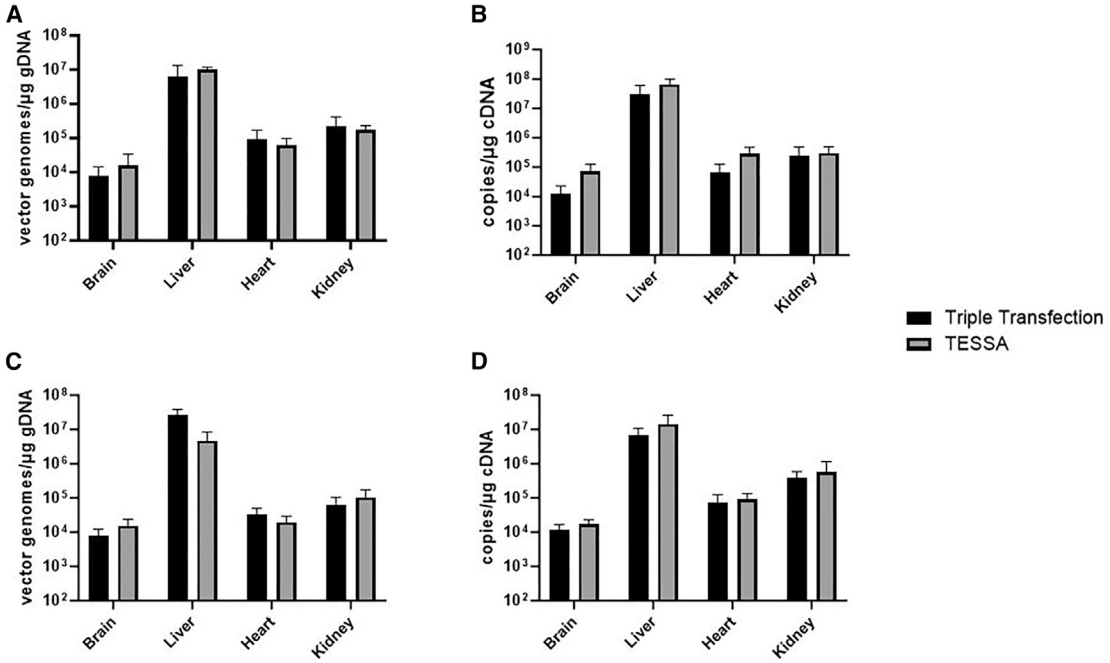

Figure 6. In vivo potency comparison across production methods

(A) *In vivo* murine potency gDNA results comparing triple transfection- and TESSA-produced AAV5-sc-GOI2 dosed at 5E13 vg/kg. (B) *In vivo* murine potency cDNA results comparing triple transfection- and TESSA-produced AAV5-sc-GOI2 dosed at 5E13 vg/kg. (C and D) *In vivo* murine potency gDNA results comparing triple transfection- and TESSA-produced AAV5-ss-GOI3 dosed at 5E13 vg/kg (D) *In vivo* murine potency cDNA results comparing triple transfection- and TESSA-produced AAV5-ss-GOI3 dosed at 5E13 vg/kg.

the potency of the vectors produced from the TESSA platform was equivalent to that of the triple transfection system. Using an *in vitro* potency assay that assessed RNA expression from AAV-transduced HeLa RC32 cells, we found that AAV5-sc-GOI2 from the TESSA and triple transfection systems exhibited comparable potency. While the *in vitro* potency assessment is meaningful, a more relevant potency evaluation would be the comparison of the platforms *in vivo*. We conducted a comparison of the TESSA production platform and triple transfection platform *in vivo* for both AAV5-sc-GOI2 and AAV5-ss-GOI3. Ultimately, we found that the *in vivo* potency was also comparable for the TESSA-produced rAAV5 across the two different GOIs. Although AAV5-ss-GOI3 produced from TESSA showed a slightly lower *in vitro* potency compared with the triple transfection material, this result is in stark contrast with the *in vivo* potency assessment. While *in vitro* potency assays are useful in providing an approximate estimation of potency and assessment of AAV batch quality, they are not always likely to corroborate with *in vivo* potency results. This is an important observation as other production systems, such as baculovirus Sf9, which have been shown to improve rAAV production yields, exhibited a decrease in rAAV5 potency when compared with HEK293-produced rAAV.[19,20] This decrease in potency is likely related to changes in rAAV post-translational modifications between the insect and mammalian production systems, which is not an issue with TESSA-produced rAAV, as it can use the same HEK293 cell line as traditional triple transfection to maintain comparable *in vivo* potency, as our data have shown.[8,9]

In summary, the TESSA production system allows for a more than 20× boost in rAAV production using HEK293 cells. We showed that TESSA-produced rAAV has post-translational modifications that are similar to triple transfection generated rAAV. Importantly, when assessed for rAAV potency activity in cells and animals, TESSA-produced rAAV performs similar to triple transfection produced rAAV, and without a decrease in potency, which has been reported in other production systems, such as the baculovirus Sf9 system.[19,20] Future studies are needed to explore the full potential of the TESSA platform, including, but not limited to, scaling to large-scale bioreactor productions and rAAV assessment in larger animal models, particularly non-human primates.

MATERIALS AND METHODS

Animal studies

All studies and procedures were approved and conducted in compliance of the Institutional Animal Care and Use Committee of Mispro, LLC in their Durham, NC facility. C57BL/6J mice (Jax Labs) were housed in standard laboratory cages within temperature (22°C–23°C) and humidity (30%–70%) controlled rooms under a 12:12 light:dark cycle. Only male animals were used for studies.

Test article was administered at a final dose of 5×10^{13} vg/kg via tail vein injection using a 30G insulin syringe. Four weeks after dosing, mice were sacrificed, and their liver, adrenal glands, brain, and heart were collected and snap frozen for biodistribution analysis.

Generation of AAV by triple transfection

For all cell culture experiments, an HEK293-derived suspension cell line was cultured in either Expi293 Expression Medium (Thermo Fisher Scientific) or BalanCD HEK293 Media (Irvine Scientific) at 37°C and 5% CO_2, and 130 rpm within Optimum Growth flasks (Thomson). Cells were inoculated at a 0.3E+6 viable cell density and grown up for 3 days before transfection or transduction. Cells were diluted to the appropriate cell density for both the TESSA (1.5E6/mL) and triple transfection process (2E6/mL) with fresh media. Triple transfection was performed at a 5% cell culture volume using PEImax (Polysciences) with a 3:1 ratio of PEI to DNA. A total plasmid DNA amount of 0.5 μg/1E6 viable cells was used for triple transfection. At 72 h after transfection, lysis buffer containing 20% Tween 20 (VWR), 40 mM magnesium chloride (Sigma-Aldrich), and 1M Tris (Sigma-Aldrich) at pH 8.0 was added to a final concentration of 1% Tween 20, 2 mM magnesium chloride, and 50 mM Tris. Samples undergoing purification had Salt-Active Nuclease (Arcticzymes) added to a final concentration of 25 U/mL and 5 M sodium chloride (Promega) added to a final concentration of 0.5 M for digestion of nucleic acid. After salt-active nuclease treatment, the lysate was 0.2 micron filtered before affinity chromatography.

Production of AAV by TESSA Pro

HEK293 cells were cultured as described above. Rather than performing a transfection, components necessary for production of AAV were introduced to the cells by addition of TESSA-RepCap5 and either AAV5-ss-GOI1, AAV5-sc-GOI2, or AAV5-ss-GOI3. The TESSA-RepCap5 vector was purchased from OXGENE, a WuXi Advanced Therapies Company (OXGENE) and the infectious titer described in optimization experiments was calculated using the TCID50 titer provided with the product. The rAAV5 material was generated as described above and the titer was determined by ddPCR in the subsequent section. All transgenes used common constitutive promoters such as CBA (GOI 1) or CB6 (GOI 2 and GOI 3).

Purification

We purified 0.2 micron filtered, clarified lysate across POROS CaptureSelect AAVX Affinity column (ThermoFisher). The AAV was eluted via a low pH elution. The elution was collected, pooled, neutralized, and stored at 2°C–8°C overnight before anion exchange chromatography. The affinity eluate was subsequently dilute to pH 9 and loaded across a POROS 50 HQ Strong Anion Exchange Column (ThermoFisher, Rockford). Post load, the column was subjected to a sodium acetate gradient to elicit elution of the full capsid particles. The eluate was subsequently concentrated using a 100-kDa Amicon ultra centrifugal spin filter (Sigma-Aldrich) before sterile 0.2 μm filtration. All rAAV seed stocks were purified as described above.

ddPCR

Viral genome titer was determined using ddPCR. Test samples and controls were treated with an endonuclease for 30 min at 37°C. Treated samples were subjected to proteinase K digestion at 55°C for 30 min followed by a proteinase K inactivation at 95°C for 15 min. All samples and controls were serially diluted. Applicable sample dilutions were combined with Bio-Rad ddPCR Supermix (Bio-Rad) for probes (no dUTP) and a rabbit beta-globin polyadenylation signal specific primer-probe set. Following droplet generation, droplets were immediately subjected to PCR thermal cycling: 95°C for 10 min, 39 cycles of 95°C for 30 s, 60°C for 1 min, and 98°C for 10 min, followed by an indefinite hold at 4°C. Droplets detection was completed on a Bio-Rad QX200 droplet reader using FAM detection. Viral genome copies within the assay dynamic range of 100–100,000 copies per reaction were quantified.

AAV5 capsid ELISA

Capsid ELISA was run using the AAV5 Xpress ELISA from Progen (PRAAV5XP) according to the manufacturer's instructions. Samples were serially diluted in 1× assay buffer before plating. After initial incubation, biotinylated anti-AAV5 antibody was added and incubated again before the streptavidin-peroxidase conjugate addition and incubation. Following streptavidin-peroxidase conjugation, 3,3′,5,5′-tetramethylbenzidine, was added and incubated followed by the addition of kit-provided "STOP." Each incubation was 20 min at 37°C. The resulting colorimetric signal was measured at 450 nm via SpectraMax iD5 reader. Samples were correlated with the standard curve generated by the serial dilution of the standard.

SDS-PAGE gel electrophoresis

VP ratios were analyzed by SDS-PAGE and subsequent scanning densitometry. Reducing buffer consisting of 2-β mercaptoethanol (Bio-Rad) and non-reducing 4× Laemmli SDS Sample Buffer (ThermoFisher) were prepared. Test samples were diluted 1:4 in reducing buffer to a target load of 5.00E+10 vg. Diluted samples were denatured at 95°C for 5 min. After denaturation, samples were loaded onto a 4–15% Mini-PROTEAN TGX Precast Protein Gel (Bio-Rad) and separated by electrophoresis. The gel was incubated in SimplyBlue SafeStain (Invitrogen) and imaged on a ChemiDoc MP Imaging System (Bio-Rad). Scanning densitometry was conducted using Image Lab (Bio-Rad) to determine VP ratios.

Residual HEK293 host cell DNA quantification

Residual HEK293 host cell DNA was measured using the resDNA-SEQ Quantitative HEK293 DNA Kit (Thermo Fisher Scientific).

Analysis of post-translational modifications via mass spectrometry

Triplicate samples (4 μg protein per replicate) were denatured in 0.2% Rapigest (Waters) at 95°C for 10 min. Capsids were reduced and alkylated before digestion with trypsin (Promega) (1:10) for 2 h at 37°C. The Rapigest was hydrolyzed with 0.5M HCl at 37°C for 45 min followed by centrifugation at 16,000×*g* for 10 min.

We injected 20 μL of each sample onto an Acquity UPLC Peptide CSH C18 Column 1.7 μm, 2.1 × 100 mm (Waters) maintained at 60°C adapted to a Vanquish Flex liquid chromatograph (Thermo Fisher Scientific). A mobile phase consisting of 0.1% formic acid in water (mobile phase A) and 0.1% formic acid in acetonitrile (MPB) was ramped from 2 to 40% MPB over 29 min. Peptides were mass-analyzed using a Q-Exactive Orbitrap mass spectrometer (Thermo Fisher Scientific) by data-dependent acquisition operated in positive-ion mode. Sequence coverage and posttranslational modifications were identified and characterized using BioPharmaFinder software (Thermo Fisher Scientific).

In vitro potency assay

HeLaR32 cells (ATCC) were propagated in high glucose DMEM (Thermo Fisher Scientific), or DMEM, containing 10% fetal bovine serum (Corning). For experiments, 30,000 cells were added to each well of a 96-well plate in serum-free DMEM and transduced with AAV ranging from an MOI of 200,000 to 3,125. After 4 h, cells were washed and complete growth media was added. Twenty-four hours after the initiation of reverse transduction, cells were washed and processed for RNA isolation.

RNA Isolation was performed on Eppendorf epMotion 5075 and was adapted from RNAdvance Cell v2 Kit (Beckman Coulter). We added 63 μL of lysis solution to each well and incubated them for 30 min at room temperature. After incubation, the entire lysate was transferred to a 96-well deep plate for automated RNA purification. Eppendorf epMotion 5075 was used for total RNA binding to beads, DNase treatment, washing and RNA elution. RNA samples were quantified using a fluorescent based kit Invitrogen Quant-iT RNA (Thermo Fisher Scientific).

We tested 20 ng of RNA in triplicate with IDT RT-qPCR master mix (IDT) using a BioRad CFX96 instrument with the following conditions: the first cycle at 50°C for 15 min, the second cycle at 95°C for 3 min, and the third cycle (repeated 40 times) at 95°C for 10 s and 60°C for 30 s. Primers and probe for the GOI and reference gene were multiplexed in each sample reaction. The quantified level of GOI mRNA was normalized to the quantified level of reference gene mRNA for every MOI within each condition. Delta-delta Ct was used to plot the relative change across the samples at each MOI. The ratio of normalized expression—the relative potency—is then calculated for every MOI for each test condition (test sample(s) to reference). The *in vitro* potency of the positive control and test sample(s) is reported as the average of the relative potency across the MOI.

RNA/DNA isolation from animal tissue

Tissue samples from mice were collected in 4mm punches, including brain, liver, heart, and kidney. Samples were stored in 2mL Eppendorf safe-lock lysis tubes (Eppendorf) with a Qiagen 5-mm steel bead (Qiagen) at −80°C until sample processing. The tissues were homogenized with RNAdvance tissue lysis buffer and proteinase K at 37°C for 25 min. Samples were then clarified at 12,000×*g*. Clarified lysate was transferred to a 96-well plate for loading onto Eppendorf epMotion 5075t. The genomic DNA (gDNA) and RNA samples were quantified using a fluorescent based kit Invitrogen Quant-iT gDNA and RNA (#Q33130 and Q33140 Thermo Fisher Scientific).

PCR assessment of vector genomes and transgene RNA

RNA was reverse transcribed to cDNA using Qiagen RT2 first strand kit (#330404 Qiagen). A custom qPCR assay was designed for vector genomes or GOI transgene with final concentrations of 500 nM for the forward primer, 500 nM for the reverse primer, and 125 nM for the probe. Standard curves were created using a DNA fragment from 5e6 copies per reaction to 5e1 copies per reaction. We mixed 4 mL of template (gDNA [100 ng total]/cDNA[10 ng total]) in a final volume of 20 mL. Samples were tested in triplicate with IDT master mix (#1055771 IDT) using a BioRad CFX96 instrument with the following conditions: first cycle at 95°C for 3 min and a second cycle (repeated 40 times) at 95°C for 10 s and 60°C for 30 s. Vector genome and transgene copies per reaction were determined by comparison with the standard. Copies per microgram were then determined by using the following formula:

$$Copies\ per\ \mu g\ =\ Copies\ per\ rxn \times \left(\frac{1\ \mu g}{\mu g\ of\ gDNA\ or\ cDNA\ input}\right).$$

DATA AND CODE AVAILABILITY

The data from this study are available upon request from the corresponding author, M.K.R.

ACKNOWLEDGMENTS

This work was funded by BridgeBio Gene Therapy LLC, and all authors own equity interests in this organization. The authors would like to thank Weiheng Su, Armin Hekele, and Mary Herrick for their thoughtful review of the manuscript.

AUTHOR CONTRIBUTIONS

M.K.R. and P.W. conceptualized the study. D.S. provided guidance and aided in experiment design. M.K.R. and P.W. completed most of the experiments. D.S. and J.R. carried out the potency assays and *in vivo* biodistribution. A.S. conducted the mass spectrometry and subsequent analysis. M.K.R, P.W., A.S., J.R., and D.S. wrote the manuscript. D.S. and C.B. provided mentorship.

DECLARATION OF INTERESTS

The authors declare no competing interests.

SUPPLEMENTAL INFORMATION

Supplemental information can be found online at https://doi.org/10.1016/j.omtm.2024.101320.

REFERENCES

1. Au, H.K.E., Isalan, M., and Mielcarek, M. (2021). Gene Therapy Advances: A Meta-Analysis of AAV Usage in Clinical Settings. Front. Med. *8*, 809118. https://doi.org/10.3389/fmed.2021.809118.
2. Srivastava, A. (2016). In vivo tissue-tropism of adeno-associated viral vectors. Curr. Opin. Virol. *21*, 75–80. https://doi.org/10.1016/j.coviro.2016.08.003.
3. Guan, J.S., Chen, K., Si, Y., Kim, T., Zhou, Z., Kim, S., Zhou, L., and Liu, X.M. (2022). Process improvement of adeno-associated virus (AAV) production. Front. Chem. Eng. *4*, 830421. https://doi.org/10.3389/fceng.2022.830421.

4. Dickerson, R., Argento, C., Pieracci, J., and Bakhshayeshi, M. (2021). Separating Empty and Full Recombinant Adeno-Associated Virus Particles Using Isocratic Anion Exchange Chromatography. Biotechnol. J. *16*, e2000015. https://doi.org/10.1002/biot.202000015.

5. Lavoie, R.A., Zugates, J.T., Cheeseman, A.T., Teten, M.A., Ramesh, S., Freeman, J.M., Swango, S., Fitzpatrick, J., Joshi, A., Hollers, B., et al. (2023). Enrichment of adeno-associated virus serotype 5 full capsids by anion exchange chromatography with dual salt elution gradients. Biotechnol. Bioeng. *120*, 2953–2968. https://doi.org/10.1002/bit.28453.

6. Kurasawa, J.H., Park, A., Sowers, C.R., Halpin, R.A., Tovchigrechko, A., Dobson, C.L., Schmelzer, A.E., Gao, C., Wilson, S.D., and Ikeda, Y. (2020). Chemically Defined, High-Density Insect Cell-Based Expression System for Scalable AAV Vector Production. Mol. Ther. Methods Clin. Dev. *19*, 330–340. https://doi.org/10.1016/j.omtm.2020.09.018.

7. Clément, N., Knop, D.R., and Byrne, B.J. (2009). Large-scale adeno-associated viral vector production using a herpesvirus-based system enables manufacturing for clinical studies. Hum. Gene Ther. *20*, 796–806. https://doi.org/10.1089/hum.2009.094.

8. Rumachik, N.G., Malaker, S.A., Poweleit, N., Maynard, L.H., Adams, C.M., Leib, R.D., Cirolia, G., Thomas, D., Stamnes, S., Holt, K., et al. (2020). Methods Matter: Standard Production Platforms for Recombinant AAV Produce Chemically and Functionally Distinct Vectors. Mol. Ther. Methods Clin. Dev. *18*, 98–118. https://doi.org/10.1016/j.omtm.2020.05.018.

9. Giles, A., Lock, M., Chen, S.J., Turner, K., Wesolowski, G., Prongay, A., Petkov, B.N., Olagbegi, K., Yan, H., and Wilson, J.M. (2023). Significant Differences in Capsid Properties and Potency Between Adeno-Associated Virus Vectors Produced in Sf9 and HEK293 Cells. Hum. Gene Ther. *34*, 1003–1021. https://doi.org/10.1089/hum.2022.116.

10. Su, W., Patrício, M.I., Duffy, M.R., Krakowiak, J.M., Seymour, L.W., and Cawood, R. (2022). Self-attenuating adenovirus enables production of recombinant adeno-associated virus for high manufacturing yield without contamination. Nat. Commun. *13*, 1182. https://doi.org/10.1038/s41467-022-28738-2.

11. Mendes, J.P., Fernandes, B., Pineda, E., Kudugunti, S., Bransby, M., Gantier, R., Peixoto, C., Alves, P.M., Roldão, A., and Silva, R.J.S. (2022). AAV process intensification by perfusion bioreaction and integrated clarification. Front. Bioeng. Biotechnol. *10*, 1020174. https://doi.org/10.3389/fbioe.2022.1020174.

12. Zhang, X., Jin, X., Liu, L., Zhang, Z., Koza, S., Yu, Y.Q., and Chen, W. (2021). Optimized Reversed-Phase Liquid Chromatography/Mass Spectrometry Methods for Intact Protein Analysis and Peptide Mapping of Adeno-Associated Virus Proteins. Hum. Gene Ther. *32*, 1501–1511. https://doi.org/10.1089/hum.2021.046.

13. Chung, C.H., Murphy, C.M., Wingate, V.P., Pavlicek, J.W., Nakashima, R., Wei, W., McCarty, D., Rabinowitz, J., and Barton, E. (2023). Production of rAAV by plasmid transfection induces antiviral and inflammatory responses in suspension HEK293 cells. Mol. Ther. Methods Clin. Dev. *28*, 272–283. https://doi.org/10.1016/j.omtm.2023.01.002.

14. Ellis, B.L., Hirsch, M.L., Barker, J.C., Connelly, J.P., Steininger, R.J., 3rd, and Porteus, M.H. (2013). A survey of ex vivo/*in vitro* transduction efficiency of mammalian primary cells and cell lines with Nine natural adeno-associated virus (AAV1-9) and one engineered adeno-associated virus serotype. Virol. J. *10*, 74. https://doi.org/10.1186/1743-422X-10-74.

15. Kohlbrenner, E., Aslanidi, G., Nash, K., Shklyaev, S., Campbell-Thompson, M., Byrne, B.J., Snyder, R.O., Muzyczka, N., Warrington, K.H., Jr., and Zolotukhin, S. (2005). Successful production of pseudotyped rAAV vectors using a modified baculovirus expression system. Mol. Ther. *12*, 1217–1225. https://doi.org/10.1016/j.ymthe.2005.08.018.

16. Mietzsch, M., Casteleyn, V., Weger, S., Zolotukhin, S., and Heilbronn, R. (2015). OneBac 2.0: Sf9 Cell Lines for Production of AAV5 Vectors with Enhanced Infectivity and Minimal Encapsidation of Foreign DNA. Hum. Gene Ther. *26*, 688–697. https://doi.org/10.1089/hum.2015.050.

17. Warrington, K.H., Jr., Gorbatyuk, O.S., Harrison, J.K., Opie, S.R., Zolotukhin, S., and Muzyczka, N. (2004). Adeno-associated virus type 2 VP2 capsid protein is nonessential and can tolerate large peptide insertions at its N terminus. J. Virol. *78*, 6595–6609. https://doi.org/10.1128/JVI.78.12.6595-6609.2004.

18. Giles, A.R., Sims, J.J., Turner, K.B., Govindasamy, L., Alvira, M.R., Lock, M., and Wilson, J.M. (2018). Deamidation of Amino Acids on the Surface of Adeno-Associated Virus Capsids Leads to Charge Heterogeneity and Altered Vector Function. Mol. Ther. *26*, 2848–2862. https://doi.org/10.1016/j.ymthe.2018.09.013.

19. Urabe, M., Nakakura, T., Xin, K.Q., Obara, Y., Mizukami, H., Kume, A., Kotin, R.M., and Ozawa, K. (2006). Scalable generation of high-titer recombinant adeno-associated virus type 5 in insect cells. J. Virol. *80*, 1874–1885. https://doi.org/10.1128/JVI.80.4.1874-1885.2006.

20. Kondratov, O., Marsic, D., Crosson, S.M., Mendez-Gomez, H.R., Moskalenko, O., Mietzsch, M., Heilbronn, R., Allison, J.R., Green, K.B., Agbandje-McKenna, M., and Zolotukhin, S. (2017). Direct Head-to-Head Evaluation of Recombinant Adeno-associated Viral Vectors Manufactured in Human versus Insect Cells. Mol. Ther. *25*, 2661–2675. https://doi.org/10.1016/j.ymthe.2017.08.003.